INSTITUTE OF PHYSICS PUBLISHING JOURNAL OF OPTICS A: PURE AND APPLIED OPTICS

J. Opt. A: Pure Appl. Opt. **5** (2003) S293–S297 PII: S1464-4258(03)56270-5

Gradient parameter and axial and field rays in the gradient-index crystalline lens model

M V Pérez, C Bao, M T Flores-Arias, M A Rama and C Gómez-Reino

Departamento de Física Aplicada, Facultad de Física y Escuela Universitaria de Óptica y Optometría, Campus Sur, Universidade de Santiago de Compostela, E-15782 Santiago de Compostela, Spain

E-mail: facgrc@usc.es

Received 14 November 2002, accepted for publication 6 June 2003
Published 22 August 2003
Online at stacks.iop.org/JOptA/5/S293

Abstract
Gradient-index models of the human lens have received wide attention in optometry and vision sciences for considering how changes in the refractive index profile with age and accommodation may affect refractive power. This paper uses the continuous asymmetric bi-elliptical model to determine gradient parameter and axial and field rays of the human lens in order to study the paraxial propagation of light through the crystalline lens of the eye.

Keywords: Crystalline lens, GRIN optics

1. Introduction

The eye is the main organ for sensing light and its design is such that it is optimal for capturing light and forming an image. The eye is, in many aspects, like a camera. The optical system of the eye forms an image on the retina, whereas the camera lens forms its image on the film. The camera must be focused by changing the distance from the lens to the film. However, a change in the configuration of the crystalline human lens occurs when the eye needs to focus at different distances by accommodation. This involves alterations in curvature, thickness and refractive index of the lens. A change in the axial length of the eye is not involved.

On the other hand, the refractive index of the human lens is not constant. The index value is almost constant in the nuclear region but a decrease of index exists in the cortex of the lens. Optical modelling of the crystalline lens uses two different models: the shell and continuous gradient-index models. In the shell or laminated model, the gradient index is represented by a finite and discrete set of concentric shells, with a constant refractive index in each shell [1–3]. In the construction of such a model, it is necessary to decide the number of shells, how the refractive index varies from shell to shell, and the value of curvature of the surface of each shell. Once the shell structure is established, paraxial ray-tracing can be used to determine the lens power [4].

For the continuous gradient-index (GRIN) model the refractive index profile is represented by continuous iso-indicial surfaces. Blaker [5] was probably the first to offer a model with a continuous and smoothly varying gradient refractive index crystalline lens. The distribution was parabolic, both along the optical axis and perpendicularly in the equatorial section. Smith *et al* [6, 7] described four models pertaining to the external shape of the lens and the internal contours of refractive index. For the first two models the refractive index distribution is represented by bi-elliptical iso-indicial surfaces that are concentric with the lens surfaces. The first model assumes symmetric iso-indicial surfaces; the second an asymmetric model in which the posterior curvature of any iso-indicial surface is greater than the anterior in such a way that, at the equatorial plane of joining, the iso-indicial surface is smooth and continuous, as depicted in figure 1. Such a model has also been proposed by Jagger [8] to describe the cat lens. The third model is a modified version of the second model, in which the iso-indicial surfaces remain asymmetric elipsoids, but the surfaces of the lens are no longer iso-indicial contours. The last model is more general, being allowed any conicoid surface shape and a non-smooth joint at the equator. The second and third models provide a closest simulation to the real situation. Another approach to modelling the whole profile of the crystalline lens is that proposed by Popiolek-Masajada and Kasprzak [9], which

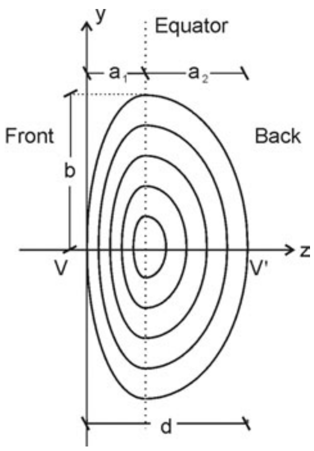

Figure 1. The refractive index distribution of the lens of the eye in the sagittal section, represented as bi-elliptical iso-indicial curves joined at the equator. For the iso-indicial curves the origin of the axes is at V.

was more fully explained by Kasprzak [10]. This involves fitting the lens profile by hyperbolic cosine functions that are, in turn, modulated by hyperbolic tangent functions. The mathematics of this approach are much more complex than the conic modelling. The aim of this paper, in the framework of the second model, is to find analytical expressions in the paraxial domain approximating the gradient parameter that characterizes the refractive index distribution and the axial and field rays that describe the light propagation, as well as the weak inhomogeneity condition, for a small variation in the gradient parameter over a wavelength distance. Knowledge of such elements should be useful for evaluating the refractive power and the cardinal points of the crystalline lens from its GRIN nature.

2. The crystalline lens gradient parameter

For the asymmetric bi-elliptical model, the refractive index profile at any point in the sagittal section of the lens can be written as a power series [4, 11–13]:

$$n(y,z) = \sum_{j=0}^{\infty} c_j f^j(y,z) \tag{1}$$

where c_j are coefficients of the power series and

$$f(y,z) = \frac{(z-a_1)^2}{a_1^2} + \frac{y^2}{b^2} \tag{2a}$$

for the front part of the lens and

$$f(y,z) = \frac{(z-a_1)^2}{a_2^2} + \frac{y^2}{b^2} \tag{2b}$$

for the back part of the lens, where a_1 and a_2 are the semi-axes along the z optical axis of the asymmetric bi-elliptical iso-indicial curves and b is the common semi-axis along the y-axis (see figure 1). $f(y,z)$ is defined so that, at the outer surface of the iso-indicial profile, it becomes unity.

If the central index is n_c and the edge index is n_e then, from equations (1) and (2), we have the following conditions:

$$n_c = c_0 \tag{3a}$$

$$n_e = \sum_{j=0}^{\infty} c_j \tag{3b}$$

and then

$$\Delta n = \sum_{j=1}^{\infty} c_j \tag{4}$$

where Δn is the difference in refractive index between the edge and the centre of the crystalline lens.

At the equator any iso-indicial curve is smooth and continuous, in such a way that the refractive index and its derivatives with respect to y of odd and even orders are given by

$$n(y,a_1) = n_f(y,z)|_{z=a_1} = n_b(y,z)|_{z=a_1} = \sum_{j=0}^{\infty} c_j \left(\frac{y}{b}\right)^{2j} \tag{5a}$$

and

$$\frac{d^p n(y,a_1)}{dy^p} = \frac{1}{b^p}\sum_{j=q}^{\infty} 2j(2j-1)\cdots(2j-p+1)c_j\left(\frac{y}{b}\right)^{2j-p} \tag{5b}$$

where $q = p/2$ for even p and $q = (p+1)/2$ for odd p and sub-indices f and b denote front and back parts of the lens, respectively.

In particular, at the centre of the equator the derivatives cancel and at the edge they reduce to

$$\left.\frac{d^p n(y,a_1)}{dy^p}\right|_{y=b} = \frac{1}{b^p}\sum_{j=q}^{\infty} 2j(2j-1)\cdots(2j-p+1)c_j. \tag{6}$$

Likewise, along the optical axis, the refractive index for the front and back parts is given, respectively, by

$$n_{0f}(z) = n_f(y,z)|_{y=0} = \sum_{j=0}^{\infty} c_j\left(\frac{z-a_1}{a_1}\right)^{2j} \tag{7a}$$

$$n_{0b}(z) = n_b(y,z)|_{y=0} = \sum_{j=0}^{\infty} c_j\left(\frac{z-a_1}{a_2}\right)^{2j} \tag{7b}$$

and the derivatives with respect to z are written as

$$\frac{d^p n_{0f}(z)}{dz^p} = \frac{1}{a_1^p}\sum_{j=q}^{\infty} 2j(2j-1)\cdots \times (2j-p+1)c_j\left(\frac{z-a_1}{a_1}\right)^{2j-p} \tag{8a}$$

$$\frac{d^p n_{0b}(z)}{dz^p} = \frac{1}{a_2^p}\sum_{j=q}^{\infty} 2j(2j-1)\cdots \times (2j-p+1)c_j\left(\frac{z-a_1}{a_2}\right)^{2j-p} \tag{8b}$$

where, again, $q = p/2$ for even p and $q = (p+1)/2$ for odd p.

In particular, at the centre all derivatives vanish while at the vertices V, V′ they verify the condition

$$\frac{d^p n_{0f}(z)/dz^p|_{z=0}}{d^p n_{0b}(z)/dz^p|_{z=d}} = (-1)^p\left(\frac{a_2}{a_1}\right)^p \tag{9}$$

where $d = a_1 + a_2$ is the thickness of the crystalline lens along the z-axis (figure 1).

To apply the well known results on GRIN optics to a crystalline lens, we can now write equation (1), for the paraxial region, as [14–16]

$$n(y, z) = n_0(z)\left[1 - \frac{g^2(z)}{2}y^2\right] \qquad (10)$$

where $n_0(z)$ is the index along the optical axis and $g(z)$ is the gradient parameter which characterizes the refractive index distribution. As we are only concerned with the GRIN nature of the crystalline lens, all terms of higher than second order in y, for the refractive index profile, are aberration terms and are rejected in the paraxial domain.

For the front part of the lens, we have

$$g_{\rm f}^2(z) = -\frac{\sum_{j=1}^{\infty} 2jc_j[\frac{z-a_1}{a_1}]^{2(j-1)}}{b^2 n_{0{\rm f}}(z)} \qquad (11a)$$

where $n_{0{\rm f}}(z)$ is given by equation (7a), and for the back part of the lens

$$g_{\rm b}^2(z) = -\frac{\sum_{j=1}^{\infty} 2jc_j[\frac{z-a_1}{a_2}]^{2(j-1)}}{b^2 n_{0{\rm b}}(z)} \qquad (11b)$$

where $n_{0{\rm b}}(z)$ is given by equation (7b).

It is clear that the gradient parameter depends on c_j (which are the coefficients of the power series in the refractive index profile), the equatorial radius b, and the index of refraction along the optical axis.

In particular, the values of the gradient parameter at the centre and the edges of the optical axis are given by

$$g_{\rm c}^2 = g_{\rm f}^2(a_1) = g_{\rm b}^2(a_1) = -\frac{2c_1}{b^2 c_0} = -\frac{2c_1}{n_{\rm c} b^2} \qquad (12a)$$

$$g_{\rm e}^2 = g_{\rm f}^2(0) = g_{\rm b}^2(d) = -\frac{2\sum_{j=1}^{\infty} jc_j}{b^2 n_{\rm e}} \qquad (12b)$$

where equations (3) have been used.

To estimate the variation in the gradient parameter along the optical axis for different values of c_j, the Gullstrand no 1 eye model for the GRIN refractive index is used. The refractive index distribution has a central and edge refractive index of 1.406 and 1.386, respectively. Figure 2 depicts $g(z)$ versus z for two, three and four coefficients of the power series in the refractive index distribution. The variation in $g(z)$ along the optical axis of the lens decreases with the number of coefficients.

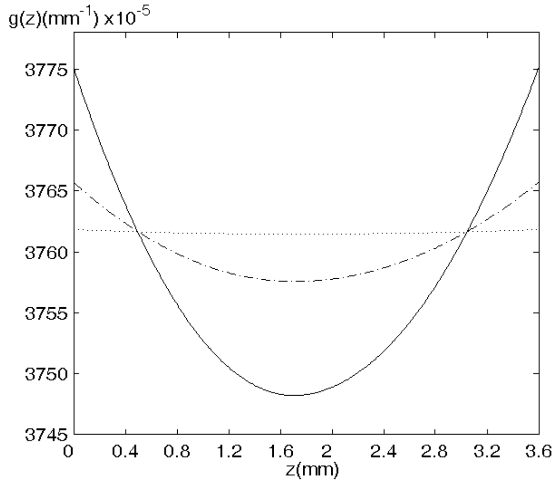

Figure 2. The variation in the gradient parameter along the axis. Calculations have been made for: $b = 4.5$ mm, $d = 3.6$ mm ($a_1 = 1.7$ mm, $a_2 = 1.9$ mm), $c_0 = 1.406$ and $c_1 = -0.02$ (solid curve); $c_1 = -0.0201$ and $c_2 = 0.0001$ (dash–dot curve); and $c_1 = -0.020\,1416$, $c_2 = 0.000\,1423$ and $c_3 = -0.000\,0007$ (dotted line).

3. Axial and field rays

It is well known that the light propagation in GRIN media can be studied by using the axial and field rays—two linearly independent solutions of the paraxial ray equation—in such a way that any paraxial ray can be expressed as a linear combination of these two rays [15, 16]

The axial and field rays in the lens can be found if the condition

$$\frac{|\dot{g}(z)|}{g^2(z)} \ll 1 \qquad (13)$$

is fulfilled for small variations in $g(z)$ over a wavelength distance (the weak inhomogeneity condition). In equation (13) a dot denotes a derivative with respect to z.

For the lens we have that

$$\frac{|\dot{g}(z)|}{g^2(z)} = \begin{cases} \frac{2b}{a_1}\left\{\left|\sum_{j=0}^{\infty} c_j\left(\frac{z-a_1}{a_1}\right)^{2j} \sum_{j=2}^{\infty} j(j-1)c_j\left(\frac{z-a_1}{a_1}\right)^{2j-3} - \sum_{j=1}^{\infty} jc_j\left(\frac{z-a_1}{a_1}\right)^{2j-2} \sum_{j=1}^{\infty} jc_j\left(\frac{z-a_1}{a_1}\right)^{2j-1}\right|\right\} \\ \quad \times\left\{\left[\sum_{j=0}^{\infty} c_j\left(\frac{z-a_1}{a_1}\right)^{2j}\right]^{1/2} \times\left[-\sum_{j=1}^{\infty} 2jc_j\left(\frac{z-a_1}{a_1}\right)^{2j-2}\right]^{3/2}\right\}^{-1} \\ \quad \text{for the front part} \\ \frac{2b}{a_2}\left\{\left|\sum_{j=0}^{\infty} c_j\left(\frac{z-a_1}{a_2}\right)^{2j} \sum_{j=2}^{\infty} j(j-1)c_j\left(\frac{z-a_1}{a_2}\right)^{2j-3} - \sum_{j=1}^{\infty} jc_j\left(\frac{z-a_1}{a_2}\right)^{2j-2} \sum_{j=1}^{\infty} jc_j\left(\frac{z-a_1}{a_2}\right)^{2j-1}\right|\right\} \\ \quad \times\left\{\left[\sum_{j=0}^{\infty} c_j\left(\frac{z-a_1}{a_2}\right)^{2j}\right]^{1/2} \times\left[-\sum_{j=1}^{\infty} 2jc_j\left(\frac{z-a_1}{a_2}\right)^{2j-2}\right]^{3/2}\right\}^{-1} \\ \quad \text{for the back part.} \end{cases} \qquad (14)$$

Figure 3 depicts the variation of equation (14) with z in the lens for two, three and four coefficients of the power series in the refractive index distribution. The more coefficients we take into account, the better condition (13) is satisfied.

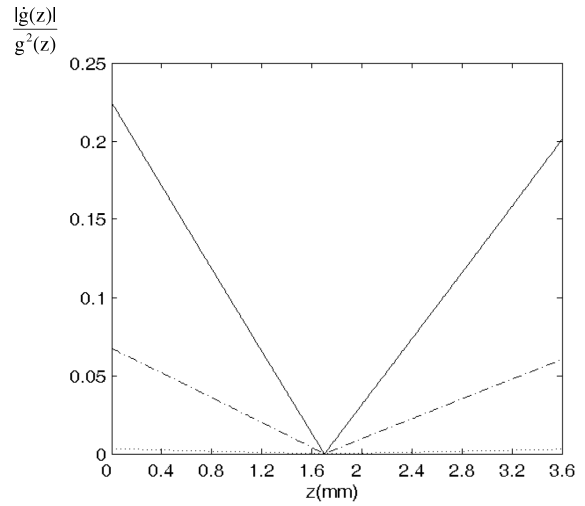

Figure 3. Condition (13) versus z. Calculations have been made for the values of figure 2.

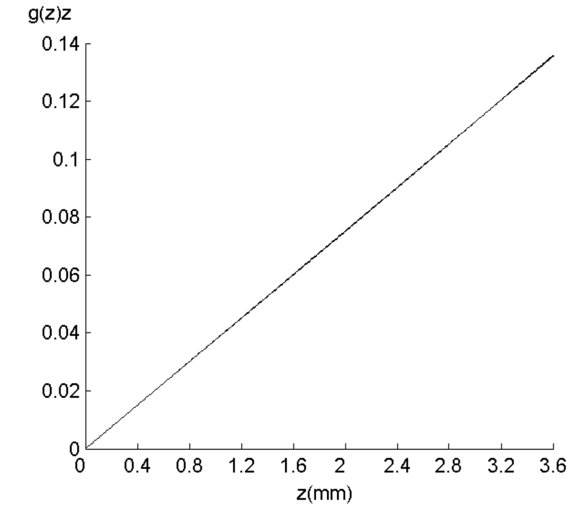

Figure 4. Variation of $g(z)z$ along the z-axis. Calculations have been made for values of figure 2. Curves for different coefficients are superimposed.

Therefore, the positions H_{a} and H_{f} and the slopes $\dot{H}_{\mathrm{a}}$ and $\dot{H}_{\mathrm{f}}$ of the axial and field rays, respectively, in the crystalline lens can be expressed as [16]

$$H_{\mathrm{af}}(z) = [g_{\mathrm{e}} g_{\mathrm{f}}(z)]^{-1/2} \sin\left[\int_0^z g_{\mathrm{f}}(z')\,\mathrm{d}z'\right] \tag{15a}$$

$$H_{\mathrm{ff}}(z) = [g_{\mathrm{e}}/g_{\mathrm{f}}(z)]^{1/2}\left\{\cos\left[\int_0^z g_{\mathrm{f}}(z')\,\mathrm{d}z'\right] + \frac{\dot{g}_{\mathrm{e}}}{2g_{\mathrm{e}}^2}\sin\left[\int_0^z g_{\mathrm{f}}(z')\,\mathrm{d}z'\right]\right\} \tag{15b}$$

$$\dot{H}_{\mathrm{af}}(z) = [g_{\mathrm{f}}(z)/g_{\mathrm{e}}]^{1/2}\left\{\cos\left[\int_0^z g_{\mathrm{f}}(z')\,\mathrm{d}z'\right] - \frac{\dot{g}_{\mathrm{f}}(z)}{2g_{\mathrm{f}}^2(z)}\sin\left[\int_0^z g_{\mathrm{f}}(z')\,\mathrm{d}z'\right]\right\} \tag{15c}$$

$$\dot{H}_{\mathrm{ff}}(z) = [g_{\mathrm{e}} g_{\mathrm{f}}(z)]^{1/2}\left\{\frac{1}{2}\left[\frac{\dot{g}_{\mathrm{e}}}{g_{\mathrm{e}}^2} - \frac{\dot{g}_{\mathrm{f}}(z)}{g_{\mathrm{f}}^2(z)}\right]\cos\left[\int_0^z g_{\mathrm{f}}(z')\,\mathrm{d}z'\right] - \left[1 + \frac{\dot{g}_{\mathrm{e}}\dot{g}_{\mathrm{f}}(z)}{4g_{\mathrm{e}}^2 g_{\mathrm{f}}^2(z)}\right]\sin\left[\int_0^z g_{\mathrm{f}}(z')\,\mathrm{d}z'\right]\right\} \tag{15d}$$

for the front part ($0 \leqslant z \leqslant a_1$) and

$$H_{\mathrm{ab}}(z) = [g_{\mathrm{e}} g_{\mathrm{b}}(z)]^{-1/2} \sin\left[\int_0^z g_{\mathrm{b}}(z')\,\mathrm{d}z'\right] \tag{15e}$$

$$H_{\mathrm{fb}}(z) = [g_{\mathrm{e}}/g_{\mathrm{b}}(z)]^{1/2}\left\{\cos\left[\int_0^z g_{\mathrm{b}}(z')\,\mathrm{d}z'\right] + \frac{\dot{g}_{\mathrm{e}}}{2g_{\mathrm{e}}^2}\sin\left[\int_0^z g_{\mathrm{b}}(z')\,\mathrm{d}z'\right]\right\} \tag{15f}$$

$$\dot{H}_{\mathrm{ab}}(z) = [g_{\mathrm{b}}(z)/g_{\mathrm{e}}]^{1/2}\left\{\cos\left[\int_0^z g_{\mathrm{b}}(z')\,\mathrm{d}z'\right] - \frac{\dot{g}_{\mathrm{b}}(z)}{2g_{\mathrm{b}}^2(z)}\sin\left[\int_0^z g_{\mathrm{b}}(z')\,\mathrm{d}z'\right]\right\} \tag{15g}$$

$$\dot{H}_{\mathrm{fb}}(z) = [g_{\mathrm{e}} g_{\mathrm{b}}(z)]^{1/2}\left\{\frac{1}{2}\left[\frac{\dot{g}_{\mathrm{e}}}{g_{\mathrm{e}}^2} - \frac{\dot{g}_{\mathrm{b}}(z)}{g_{\mathrm{b}}^2(z)}\right]\cos\left[\int_0^z g_{\mathrm{b}}(z')\,\mathrm{d}z'\right] - \left[1 + \frac{\dot{g}_{\mathrm{e}}\dot{g}_{\mathrm{b}}(z)}{4g_{\mathrm{e}}^2 g_{\mathrm{b}}^2(z)}\right]\sin\left[\int_0^z g_{\mathrm{b}}(z')\,\mathrm{d}z'\right]\right\} \tag{15h}$$

for the back part ($a_1 \leqslant z \leqslant d$), with boundary conditions

$$H_{\mathrm{af}}(0) = 0; \qquad H_{\mathrm{af}}(a_1) = H_{\mathrm{ab}}(a_1) \tag{16a}$$

$$H_{\mathrm{ff}}(0) = 1; \qquad H_{\mathrm{ff}}(a_1) = H_{\mathrm{fb}}(a_1) \tag{16b}$$

$$\dot{H}_{\mathrm{af}}(0) = 1; \qquad \dot{H}_{\mathrm{af}}(a_1) = \dot{H}_{\mathrm{ab}}(a_1) \tag{16c}$$

$$\dot{H}_{\mathrm{ff}}(0) = 0; \qquad \dot{H}_{\mathrm{ff}}(a_1) = \dot{H}_{\mathrm{fb}}(a_1) \tag{16d}$$

and with Lagrange's invariant

$$H_{\mathrm{f}\binom{\mathrm{f}}{\mathrm{b}}}(z)\dot{H}_{\mathrm{a}\binom{\mathrm{f}}{\mathrm{b}}}(z) - \dot{H}_{\mathrm{f}\binom{\mathrm{f}}{\mathrm{b}}}(z)H_{\mathrm{a}\binom{\mathrm{f}}{\mathrm{b}}}(z) = 1. \tag{17}$$

Likewise, the gradient parameter changes very slowly with z and we can expect that $g(z_1)z_1$ at z_1 is likely to be in $g(z_2)z_2$ at a very close z_2. Then, the integral in equations (15) can actually be approximated by $g(z)z$ (adiabatic approximation). Finally, $g(z)z$ is a small quantity in a crystalline lens. Figure 4 shows the variation of $g(z)z$ with z for the Gullstrand model. The maximum value of $g(z)z$ is achieved at the vertex of the back surface of the lens and is about 0.14 rad $\cong 8°$.

For these values, approximations of third and second orders for the sine and cosine are made, respectively. Thus, the position and the slope of the axial and field rays in the lens can be written as

$$H_{\mathrm{af}}(z) = \left[\frac{g_{\mathrm{f}}(z)}{g_{\mathrm{e}}}\right]^{1/2}\left[1 - \frac{g_{\mathrm{f}}^2(z)z^2}{6}\right]z \tag{18a}$$

$$H_{\mathrm{ff}}(z) = \left[\frac{g_{\mathrm{e}}}{g_{\mathrm{f}}(z)}\right]^{1/2}\left\{1 - \frac{g_{\mathrm{f}}^2(z)}{2}z^2 + \frac{\dot{g}_{\mathrm{e}} g_{\mathrm{f}}(z)}{2g_{\mathrm{e}}^2}\left[1 - \frac{g_{\mathrm{f}}^2(z)z^2}{6}\right]z\right\} \tag{18b}$$

$$\dot{H}_{\mathrm{af}}(z) = \left[\frac{g_{\mathrm{f}}(z)}{g_{\mathrm{e}}}\right]^{1/2}\left\{1 - \frac{g_{\mathrm{f}}^2(z)}{2}z^2 - \frac{\dot{g}_{\mathrm{f}}(z)}{2g_{\mathrm{f}}(z)}\left[1 - \frac{g_{\mathrm{f}}^2(z)z^2}{6}\right]z\right\} \tag{18c}$$

$$\dot{H}_{\mathrm{ff}}(z) = [g_{\mathrm{e}} g_{\mathrm{f}}(z)]^{1/2}\left\{\frac{1}{2}\left[\frac{\dot{g}_{\mathrm{e}}}{g_{\mathrm{e}}^2} - \frac{\dot{g}_{\mathrm{f}}(z)}{g_{\mathrm{f}}^2(z)}\right]\left[1 - \frac{g_{\mathrm{f}}^2(z)z^2}{2}\right] - \left[1 + \frac{\dot{g}_{\mathrm{e}}\dot{g}_{\mathrm{f}}(z)}{4g_{\mathrm{e}}^2 g_{\mathrm{f}}^2(z)}\right]\left[1 - \frac{g_{\mathrm{f}}^2(z)z^2}{6}\right]g_{\mathrm{f}}(z)z\right\} \tag{18d}$$

for the front part and

$$H_{ab}(z) = \left[\frac{g_b(z)}{g_e}\right]^{1/2}\left[1 - \frac{g_b^2(z)z^2}{6}\right]z \qquad (18e)$$

$$H_{fb}(z) = \left[\frac{g_e}{g_b(z)}\right]^{1/2}\left\{1 - \frac{g_b^2(z)}{2}z^2 + \frac{\dot{g}_e g_b(z)}{2g_e^2}\left[1 - \frac{g_b^2(z)z^2}{6}\right]z\right\} \qquad (18f)$$

$$\dot{H}_{ab}(z) = \left[\frac{g_b(z)}{g_e}\right]^{1/2}\left\{1 - \frac{g_b^2(z)}{2}z^2 - \frac{\dot{g}_b(z)}{2g_e^2}\left[1 - \frac{g_b^2(z)z^2}{6}\right]z\right\} \qquad (18g)$$

$$\dot{H}_{fb}(z) = [g_e g_b(z)]^{1/2}\left\{\frac{1}{2}\left[\frac{\dot{g}_e}{g_e^2} - \frac{\dot{g}_b(z)}{g_b^2(z)}\right]\left[1 - \frac{g_b^2(z)z^2}{2}\right] - \left[1 + \frac{\dot{g}_e\dot{g}_b(z)}{4g_e^2 g_b^2(z)}\right]\left[1 - \frac{g_b^2(z)z^2}{6}\right]g_b(z)z\right\} \qquad (18h)$$

for the back part.

We conclude that, under above conditions, the paraxial light propagation in the lens is described by the ray-transfer matrix, or ABCD matrix, as [2, 17, 18]

$$\begin{pmatrix} y(z) \\ \dot{y}(z) \end{pmatrix} = \begin{pmatrix} H_{f\binom{f}{b}}(z) & H_{a\binom{f}{b}}(z) \\ \dot{H}_{f\binom{f}{b}}(z) & \dot{H}_{a\binom{f}{b}}(z) \end{pmatrix}\begin{pmatrix} y_0 \\ \dot{y}_0 \end{pmatrix} \qquad (19)$$

where y_0 and $\dot{y}_0$ are, respectively, the position and slope of a ray at the input of the front part of the lens and $\overset{(\cdot)}{H}_{f\binom{f}{b}}$ and $\overset{(\cdot)}{H}_{a\binom{f}{b}}$ are given by equations (18). Solutions of this equation express the position $y(z)$ and the slope $\dot{y}(z)$ of the paraxial ray at any point in the lens as a linear combination of the axial and field rays.

Figure 5 shows axial and field ray-tracing in a crystalline lens for different coefficients. The axial ray describes a quasi-linear trajectory, and a very weak dependence on the number of coefficients is shown. However, the field's ray trajectory is a continuous curve depending on the coefficients.

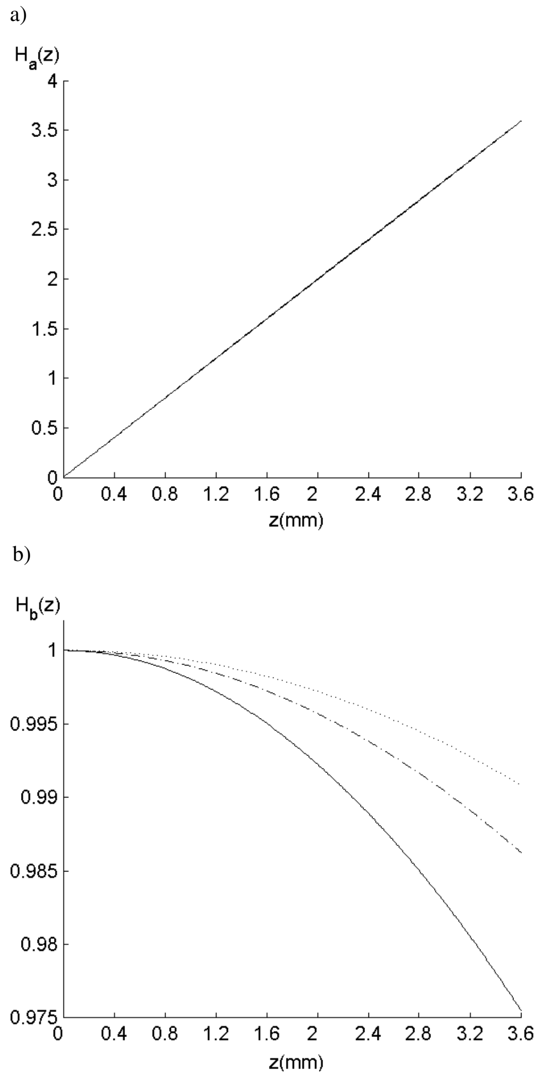

Figure 5. Axial (a) and field (b) rays in a GRIN crystalline lens with parallel faces. Calculations have been made for values of figure 2. Note that in (a) all curves for different coefficients are superimposed.

4. Conclusions

In this paper we have studied light propagation through a crystalline lens by paraxial rays, assuming the continuous gradient-index model. The axial and field rays and the gradient parameter have been evaluated as a prior step for obtaining, in the future, the refractive power and the cardinal elements of the crystalline lens in the framework of the GRIN optics.

Acknowledgment

This work was supported by the Ministerio de Ciencia y Tecnología, Spain, under contract TIC99-0489.

References

[1] Pomerantzeff O, Pankratov M, Wang G J and Dufault P 1984 *Am. J. Optom. Physiol. Opt.* **61** 166–76
[2] Raasch T and Lakshminarayanan V 1989 *Ophthalmic Physiol. Opt.* **9** 61–5
[3] Al-Ahdali I H and El-Messiery M A 1995 *Appl. Opt.* **34** 5738–45
[4] Atchison D A and Smith G 1995 *Vis. Res.* **35** 2529–38
[5] Blaker J W 1980 *J. Opt. Soc. Am.* **70** 220–3
[6] Smith G, Pierscionek B K and Atchison D A 1991 *Ophthalmic Physiol. Opt.* **11** 359–69
[7] Smith G 2003 *Clin. Exp. Optom.* **86** 3–18
[8] Jagger W S 1990 *Vis. Res.* **30** 723–38
[9] Popiolek-Masajada A and Kasprzak H T 1999 *Optom. Vis. Sci.* **76** 720–7
[10] Kasprzak H T 2000 *Ophthalmic Physiol. Opt.* **20** 31–43
[11] Nakao S, Ono T, Nagata R and Iwata K 1969 *Japan J. Clin. Ophthalmol.* **23** 903–6
[12] Pierscionek B K and Chang D Y C 1989 *Optom. Vis. Sci.* **66** 822–9
[13] Smith G, Pierscionek B K and Atchison D A 1991 *Opthalmic Physiol. Opt.* **11** 359–69
[14] Marchand E W 1978 *Gradient Index Optics* (New York: Academic)
[15] Luneburg R K 1964 *Mathematical Theory of Optics* (Berkeley, CA: University of California Press)
[16] Gómez-Reino C 1992 *Int. J. Optoelectron.* **7** 607–80
[17] Rosenblum W M and Christensen J L 1974 *Am. J. Optom. Physiol. Opt.* **51** 961–8
[18] Rosenblum W M, Blaker J W and Block M G 1988 *Am. J. Optom. Physiol. Opt.* **65** 661–5